


# Coefficients in Taylor's law increase with the time scale of water clarity measurements in a global suite of lakes

Max R. Glines<sup>1</sup>  | Renata C. H. Amancio<sup>2</sup> | Mikkel René Andersen<sup>3</sup> | Helen Baulch<sup>4</sup> | Ludmila S. Brighenti<sup>5</sup> | Hannah E. Chmiel<sup>6,7</sup> | Joel E. Cohen<sup>8,9,10</sup> | Elvira de Eyto<sup>11</sup> | Oxana Erina<sup>12</sup> | Heidrun Feuchtmayr<sup>13</sup> | Giovanna Flaim<sup>14</sup> | Andrea Giudici<sup>15</sup> | David P. Hamilton<sup>16</sup> | Yannick Huot<sup>17</sup> | Michael R. Kelly<sup>1,18</sup> | Seán Kelly<sup>19</sup> | Alo Laas<sup>20,21</sup> | Christopher McBride<sup>22</sup> | Camille Minaudo<sup>6</sup> | Jose Fernandes Bezerra Neto<sup>2</sup> | Katy Nugent<sup>4</sup> | César Ordóñez<sup>23</sup> | Marie-Elodie Perga<sup>24</sup> | Brian Reid<sup>25</sup> | Caren Scott<sup>26</sup> | Peter A. U. Staehr<sup>27</sup> | Denise Tonetta<sup>28</sup> | Danielle Wain<sup>29</sup> | Nicole K. Ward<sup>30</sup> | Kevin C. Rose<sup>1</sup>

## Correspondence

Max R. Glines, Department of Biological Sciences, Rensselaer Polytechnic Institute, Troy, NY 12180, USA.  
Email: [max.glines@gmail.com](mailto:max.glines@gmail.com)

Editor: Puni D Jeyasingh

## Abstract

Identifying the scaling rules describing ecological patterns across time and space is a central challenge in ecology. Taylor's law of fluctuation scaling, which states that the variance of a population's size or density is proportional to a positive power of the mean size or density, has been widely observed in population dynamics and characterizes variability in multiple scientific domains. However, it is unclear if this phenomenon accurately describes ecological patterns across many orders of magnitude in time, and therefore links otherwise disparate observations. Here, we use water clarity observations from 10,531 days of high-frequency measurements in 35 globally distributed lakes, and lower-frequency measurements over multiple decades from 6342 lakes to test this unknown. We focus on water clarity as an integrative ecological characteristic that responds to both biotic and abiotic drivers. We provide the first documentation that variations in ecological measurements across diverse sites and temporal scales exhibit variance patterns consistent with Taylor's law, and that model coefficients increase in a predictable yet non-linear manner with decreasing observation frequency. This discovery effectively links high-frequency sensor network observations with long-term historical monitoring records, thereby affording new opportunities to understand and predict ecological dynamics on time scales from days to decades.

## KEYWORDS

ecological variability, lakes, light attenuation, Taylor's law, water clarity

## INTRODUCTION

Characterizing variability in time and space is essential for understanding diverse ecological phenomena, including the stability and predictability of ecosystem properties and the potential for regime shifts (Cohen, 2014; Collins et al., 2018; Scheffer et al., 2001; Soranno

et al., 2019). However, patterns of ecological variability are often thought to be unique to a specific spatial or temporal scale and have corresponding unique causes and consequences (Levin, 1992). Understanding factors that regulate variability across scales, as well as identifying possible scale-invariant phenomena, is a key challenge in macrosystems ecology (Rose et al., 2017). Such

a predictive scaling relationship would provide a missing link between increasingly available high-frequency datasets and long-term infrequent observations, thereby improving forecasting capacity in an era of rapid global environmental change (Heino et al., 2021).

Taylor's law, also referred to as fluctuation scaling, has traditionally been applied to understand variability in the size or density of biological populations, but has also been observed in a wide variety of spatial and temporal studies in many disciplines (Eisler et al., 2008; Taylor, 1961, 2019). As originally proposed, Taylor's law asserts that, in many populations, fluctuations in population sizes are proportional to some power of average population size:

$$\sigma^2 = a\mu^b \quad (1)$$

where  $\sigma^2$  is the variance,  $\mu$  is the mean population size, and  $a$  and  $b$  are positive constants (Taylor, 1961). Thus,  $b$  equals the percentage increase in the variance  $\sigma^2$  associated with a 1% increase in the mean  $\mu$ . One interpretation of Taylor's law is that the exponent  $b$  represents the amount of spatial or temporal clustering or aggregation, with higher values of  $b$  signifying more clustering or less synchrony over space and time (Giometto et al., 2015). Similarly, though not as extensively studied in the literature, increases in the coefficient  $a$  correspond to greater variability over time or space, uniformly for every value of the mean  $\mu$ .

Understanding how coefficients in Taylor's law change with observation frequency may make it possible to understand and predict ecological variability across large temporal scales. However, it is currently unclear what regulates  $b$  for many ecological variables, or if this coefficient exhibits discernible patterns across observational frequencies. Many explanations such as density dependence, social behaviour, and species interactions have been invoked to explain patterns in  $b$  in populations (Kilpatrick & Cruz, 2014; Perry, 1994; Taylor & Taylor, 1977). However, the large variety of possible drivers has also led to hypotheses that several process-independent explanations may exist (Cohen, 2019; Cohen & Xu, 2015; Giometto et al., 2015; Xiao et al., 2015).

Analysis of water clarity measurements that span many orders of magnitude of time and space may reveal how Taylor's law coefficients change as a function of temporal and spatial scale of observation. Water clarity is a key indicator of ecological state and overall lake water quality, regulates a broad range of biological and physical behaviours in ecosystems, and is responsive to both biotic and abiotic drivers such as phytoplankton biomass, dissolved organic matter, and suspended solids (Adrian et al., 2009; Kirk, 1994; Williamson et al., 2009). High-frequency (i.e., sub-daily) water clarity measurements are available from sensors deployed on many waterbodies around the world. When compared across diverse sites, ecological sensor networks and the high-frequency measurements they generate may permit the

characterization of variability across several orders of magnitude in both time and space (Rose et al., 2016; Rusak et al., 2018). However, the relative youth of ecological sensor networks prohibits their application to understanding patterns at longer time scales. Complementing sensor networks, low-frequency measurements of water clarity have been made for many decades, and over a century in some cases (Lottig et al., 2014). Integrating in situ high-frequency environmental measurements with more traditional long-term monitoring could make it possible to characterize ecological variability from days to decades, and to predict variability at one temporal scale from measurements made at another (Meinson et al., 2016; Rose et al., 2016).

Here, we sought to determine if variability in water clarity was consistent with Taylor's law across a wide range of lakes and temporal scales, and if so, the degree to which coefficients describing the relationship between mean and variance in water clarity exhibited consistent changes across temporal scales. Using high-frequency (daily-averaged) light measurements from 35 lakes across the globe (Figure S1; Table 1), we calculated the variance and mean for each lake using moving windows ranging from 2 to 61 days. Complementing these high-frequency measurements, we used a large US national-scale long-term dataset to calculate the mean and variance in water clarity for over 6000 lakes with a median sampling duration of 12 years (range: 61 days to 92 years). We examined how Taylor's law coefficients changed with a time window of increasing duration, and if the relationship was consistent between days and decades of data. We hypothesized that  $a$  and  $b$  would increase with decreasing sampling frequency, consistent with greater possible variability across space and time when water clarity was observed at longer time-steps. Finally, we examined the magnitude of typical changes in water clarity in relation to ecological processes and sampling design.

## MATERIALS AND METHODS

### Study sites

We obtained in situ light measurements from 35 globally distributed lakes (Figure S1). Overall, there was some bias toward Northern hemisphere lakes, with eleven lakes in North America, eighteen in Europe, four in South America, and two in New Zealand (Table 1). Data were obtained from paired high-frequency sensors (Table S1) or vertical profilers measuring light at least hourly for a duration of at least 1 month. However, one lake with a shorter duration of data was included (Hawksbury Lagoon, 12 days of data) because it expanded the range of average light attenuation ( $K_d$ ,  $\text{m}^{-1}$ ) values across all the lakes. Sensor types and deployment depths varied, but most lakes used either Onset (seventeen lakes) or LI-COR sensors (fifteen lakes; see Table 1). NEON data

TABLE 1 Lakes used in the study.

Lake name	Sensor	Sample period (min)	Days used	Lat.	Lon.	Surface area (km <sup>2</sup> )	Mean depth (m)	Max depth (m)	Water residence time (years)	Trophic state	Mixing regime	Variance (m <sup>-2</sup> )	Mean (m <sup>-1</sup> )
Altahey Pond	Odyssey	10	44	54.024	-9.595	0.001	1.2	2.0	NA	D	Poly	0.18	4.6
Barco	LI-COR	1	490	29.676	-82.009	0.12	4.3	7.1	NA	O	Iso	0.082	1.5
Bleham Tarn	LI-COR	4	82	54.395	-2.980	0.11	6.8	14.5	0.1	M-E	Mono	0.024	1.2
Buffalo Pound	LI-COR	10	398	50.601	-105.412	30	3.0	4.5	1.0	E	Poly	7.3	4.0
Carioca	Onset	15	961	-19.75	-42.6	0.14	4.8	11.8	Endorheic	M	Poly	0.26	1.4
Castle	Onset	10	654	55.934	12.303	0.22	3.5	9.0	0.5	E	Di	1.0	2.1
Chavannes	Onset	10	35	46.333	7.086	0.06	10.6	30.0	0.9	M	Metro	7.8×10 <sup>-3</sup>	0.39
Cochrane	Onset	10	923	-47.175	-72.201	299	102.0	460	26.7	O	NA	6.6×10 <sup>-4</sup>	0.12
Dom Helvecio	Onset	15	198	-19.76	-42.58	5.3	11.3	39.2	Endorheic	O	Mono	0.041	0.58
Feeagh	Onset	30	176	53.943	-9.577	4.0	14.5	46.0	0.5	D	Mono	0.065	1.38
Geneva	LI-COR	1	409	46.500	6.661	580	154	309	11	O	Mono	7.0×10 <sup>-3</sup>	0.23
George	LI-COR	1	183	43.568	-73.642	114	18.0	58.0	7.4	O	Di	2.6×10 <sup>-3</sup>	0.31
Giles	LI-COR	1	335	41.376	-75.093	0.48	10.1	24	NA	O	Di	9.1×10 <sup>-3</sup>	0.50
Glubokoe	Onset	15	46	55.753	36.505	0.59	9.3	32.0	NA	M	NA	8.2×10 <sup>-3</sup>	0.28
Great Pond	LI-COR	15	417	44.542	-69.845	35	6.4	21.0	1.9	M	Di	8.8×10 <sup>-4</sup>	0.21
Gribsoe	Onset	10	238	55.985	12.303	0.09	4.8	11.0	2.1	D	Di	0.081	2.3
Hampen	Onset	10	223	56.018	9.392	0.66	4.3	13.0	1.4	M	Di	7.5×10 <sup>-3</sup>	0.72
Hawksbury Lagoon	LI-COR	15	12	-45.604	170.674	0.41	0.4	0.7	0.1	H	Poly	75	15
Lioson	Onset	10	35	46.386	7.129	0.07	11.5	28.5	0.9	O	Di	8.4×10 <sup>-4</sup>	0.24
Montjoie	Sea-Bird	60	29	45.409	-72.100	3.4	5.4	22.3	1.7	M-O	Di	0.016	1.1
Nohipalo Mustjärv	Onset	10	199	57.931	27.342	0.22	3.9	8.9	0.3	D	Di	0.53	3.3
Muzelle	LI-COR	30	116	44.951	6.097	0.09	12.0	18.0	0.4	O	Di	7.4×10 <sup>-3</sup>	0.23
Peri	Onset	15	356	-27.716	-48.533	5.0	4.2	11.0	NA	M	Iso	0.15	1.3
Prairie Lake	LI-COR	1	170	47.159	-99.114	0.23	NA	3.1	NA	E	Poly	3.9	4.4
Prairie Pothole	LI-COR	1	139	47.130	-99.251	0.10	NA	2.0	NA	E	Poly	4.7	6.0
Saadjärv	Onset	15	185	58.539	26.659	7.2	8.0	25.0	0.1	M	Di	4.0×10 <sup>-3</sup>	0.39
Soppen	Onset	10	119	47.090	8.080	0.25	11.4	26.0	4.0	E	NA	0.064	0.43
Suggs	LI-COR	1	158	29.687	-82.016	0.73	2.5	5.7	NA	M	Iso	2.0	4.0
Sunapee	Onset	10	121	43.394	-72.053	17	11.3	32.0	0.7	O	Di	0.25	1.2
Toolik	LI-COR	1	65	68.631	-149.611	1.5	7.0	25.0	0.5	O	Di	0.61	2.6
Tovel	Onset	30	261	46.261	30.949	0.38	19.0	39.0	<1	O	Di	1.1×10 <sup>-3</sup>	0.16
Nohipalo Valgjärv	Onset	10	584	57.941	27.347	0.07	6.2	12.5	Seepage	O	Di	0.011	0.71

(Continues)

TABLE 1 (Continued)

Lake name	Sensor	Sample period (min)	Days used	Lat.	Lon.	Surface area (km <sup>2</sup> )	Mean depth (m)	Max depth (m)	Water residence time (years)	Trophic state	Mixing regime	Variance (m <sup>-2</sup> )	Mean (m <sup>-1</sup> )
Vörtsjärv	LI-COR	15	77	58.130	26.089	270	2.8	6.0	1.0	E	Poly	0.99	2.7
Waikaremoana	Apogee	15	1549	-38.760	176.100	49	76.0	256	9.7	O	Di	1.8×10 <sup>-4</sup>	0.19
Windermere	LI-COR	4	67	54.380	-2.934	6.7	16.7	42.0	0.17–1	M	Mono	5.7×10 <sup>-3</sup>	0.56

Note: Latitude (Lat.) and longitude (Lon.) are in decimal degrees. Trophic state is indicated as oligotrophic (O), meso-oligotrophic (M-O), mesotrophic (M), meso-eutrophic (M-E), eutrophic (E), or hypertrophic (H). Mixing regime is described as monomictic (Mono), dimictic (Di), meromictic (Mero), polymictic (Poly), or isothermal (Iso).

was obtained from the NEON data portal for five sites (NEON, 2020a, 2020b).

In addition to the high-frequency data, lower-frequency water clarity data were obtained from the US Water Quality Portal (WQP) (Read et al., 2017) by downloading all recorded Secchi depth measurements for all lakes, reservoirs, and impoundments. The data retrieval returned over 1.5 million observations from an initial total of 60,363 lakes, nearly all of which are in the United States.

## Light attenuation calculation

To convert light measurements from paired sensors into light attenuation, we used the following equation (Kirk, 1994):

$$K_d = \frac{1}{z_2 - z_1} \ln \frac{E_d(z_1)}{E_d(z_2)} \quad (2)$$

where  $E_d(z)$  is the measurement of downward irradiance at depth  $z$  and  $z_2 > z_1$ . In the cases where more than 2 underwater light sensors or a vertical profiler were used (16 lakes),  $K_d$  was calculated as the slope of the fitted regression line of  $\ln(E_d)$  versus depth. Light measurements (Table S1) were obtained as PAR ( $\mu\text{mol}/\text{m}^2/\text{s}$ ), Lux (lumens/ $\text{m}^2$ ), or wavelength-specific measurements ( $\mu\text{W}/\text{cm}^2/\text{nm}$ ). Although Lux and PAR both span 400–700 nm in the electromagnetic spectrum, they are not equivalent spectra. While Lux can be converted to PAR by calibration using in situ measurements (Long et al., 2012), only 4 of the 17 lakes using Lux measurements had this conversion available. Therefore, Lux measurements were not converted to PAR for the purpose of  $K_d$  calculation. A detailed treatment of potential limitations and assumptions on sensor design and deployment is included in the supplemental section of this paper. For comparison, wavelength-specific measurements were converted to PAR as the sum of all light measurements between 400 and 700 nm before calculating  $K_d$ .

To ensure calculations were minimally influenced by the effects of sun angle and low-light conditions, we only used light measurements taken within 3 h of local solar noon. Generally, removing data points outside of this time window resulted in a small shift in the magnitude of the time series (Figure S2). While sun angle will impact light attenuation based on season and latitude (Kirk, 1994), this was not found to affect daily rates of change, and the effects of seasonal sun angle were not considered in this analysis, except for the consideration of albedo when necessary. Additional discussion of the effects of sun angle on the data is included in the supplemental text. For lakes with an above-water sensor, we adjusted surface irradiance to irradiance just below the surface according to Paulson and Pegau (2001):

$$E_d^{0-} = (1 - \alpha)E_d \quad (3)$$

where  $E_d^{0-}$  is irradiance just below the surface,  $\alpha$  is albedo, and  $E_d$  is downwelling surface irradiance. We estimated albedo based on the solar zenith angle ( $\Phi_{zen}$ ) according to (Briegleb et al., 1986):

$$\alpha = \frac{1}{100} \left( \frac{2.6}{1.1 \cos(\Phi_{zen})^{1.7} + 0.065} + 15 [\cos(\Phi_{zen}) - 0.1] [\cos(\Phi_{zen}) - 0.5] [\cos(\Phi_{zen}) - 1] \right) \quad (4)$$

We calculated all values of solar zenith angle based on local time and latitude using the R package `suncalc` (v. 0.5.0).

Interferences such as wave focusing, buoy shadows, and wiper placement can affect light attenuation calculations. To reduce their effect on daily light attenuation estimates, after calculating  $K_d$  for each set of light measurements, we removed data points where the ratio of irradiance at the lower light sensor to that at the upper light sensor was outside the first and third quartile of the distribution for each day's observations (Figure S2). Data points where more irradiance was measured at the lower sensor than the upper sensor were then removed, obvious erratic measurements were manually removed (i.e., measurements where sensors were not underwater or were affected by fouling), and the remaining measurements were used to calculate light attenuation as a daily average. Days were removed from further analyses if more than 75% of the measurements within the daily 6-h window were removed by this process ( $n=443$  days), and the remaining days were used to generate a time series (Figure S3).

We calculated the euphotic depth ( $z_{eu}$ , m) as the depth of 1% irradiance using (Kirk, 1994):

$$z_{eu} = \frac{4.6}{K_d} \quad (5)$$

While euphotic depth is an apparent optical property that depends on the total irradiance and variation of  $K_d$  with depth (Kirk, 1994), this calculation presents an estimate of euphotic depth that is useful for comparing potential changes in primary production between days based solely on changes in  $K_d$  while holding all other factors constant.

We next calculated uncertainty due to sensor error in  $K_d$  as (Zheng et al., 2002):

$$u_{kd}^2 = \left( \frac{1}{z_2 - z_1} \right)^2 (u_1^2 + u_2^2) \quad (6)$$

where  $u_{kd}$  is the uncertainty in the calculated  $K_d$  and  $u_1$  and  $u_2$  are the uncertainties in the paired light sensors. Typical sensor uncertainty has been reported in the literature as 3.8% for LI-COR sensors (Long et al., 2012), and 12% for

Onset sensors (Gardner et al., 2020). We assumed sensor uncertainty was constant for the duration of the studied period, so  $u_{kd}$  depended only on the distance between paired sensors and the sensor type. For vertical profiler measurements, we assumed  $u_{kd}$  to be 3.8%.

Water clarity measurements (reported as Secchi disk depth) from the WQP dataset were filtered to include

only measurements of at least 10 cm and no greater than 30 m, and only lakes with at least 61 observations. This reduced the total number of lakes to 6342 from the WQP. We then converted all measurements into units of meters and transformed into  $K_d$  as (Padial & Thomaz, 2008):

$$K_d = 2 * SD^{-0.76} \quad (7)$$

where SD is Secchi depth. Although there is no universal transformation from Secchi depth to light attenuation, we performed this transformation for easier comparison to the high-frequency light measurements.

## Variability calculations

To test whether Taylor's law describes variability in light attenuation, we calculated the rolling mean and variance for each time series using a centered moving window ranging from 2 to 61 days. We chose 61 days as the upper limit for our analysis because not all lakes have a sufficiently long data record to allow for larger time windows, and 61 was the last window at which more than 50% of our lakes could be included. The moving window was applied individually to each point in the time series such that points were included multiple times in rolling mean and variance calculations (i.e., the time windows overlapped). To confirm that trends in  $a$  and  $b$  with respect to a changing time window were not the result of varying sample sizes (Downing, 1986), we selected only lakes with at least 30 data points available at a 61 day time scale ( $n=21$ ) and sampled 30 data points from each lake at each time scale after calculating the rolling mean and variance. We then fitted a linear regression to the log-log plot of the rolling variance vs the rolling mean for each window size across the 21 lakes (using all 30 unique sampled measurements from each lake), which was used to calculate the parameters of the power equation:

$$\sigma_t^2 = a_t \mu_t^{b_t} \quad (8)$$

where  $\sigma_t^2$  is the variance in  $K_d$  for time window  $t$  across all lakes,  $\mu_t$  is the mean  $K_d$  for time window  $t$  across all lakes, and  $a$  and  $b$  are positive constants. Calculating the rolling mean and variance for equal window sizes in each

lake and sampling an equal number of points removed the influence of the sensor deployment times on the analysis. While applying a linear regression to the log variance and log average using this method resulted in autocorrelated residuals (Xu & Cohen, 2021), we determined that was not an issue in our analysis as we are specifically looking at the effects of autocorrelation in the time window used for Taylor's law. Trends in  $a$  and  $b$  were assessed using Spearman's rank correlation. For the lakes from the WQP dataset, we simply calculated the variance and mean light attenuation across the full observation period for each lake. We also divided the WQP data by geographic region in the United States (Northeast, Southeast, Midwest, Southwest, and West; based on Read et al., 2017) and assessed the fit of Taylor's law across regions, using an ANCOVA and paired  $t$  test post hoc analysis to test for regional differences (Table S2). Similar to lakes with high-frequency sensor measurements, we sampled an equal number of points ( $n=66$ , which was the number of lakes from the region with the least data) from each region to ensure there was no sample size bias. To confirm that a linear model was the best fit for all data, we compared a linear model to polynomial models using the Akaike Information Criterion (AIC) score. AIC scores confirmed that linear models were the best fit in all cases. We also used WQP classifications to assign each lake as either a natural lake ( $n=1345$ ) or reservoir ( $n=1796$ ). We then separately calculated coefficients from Equation (1) for each lake type and used ANCOVA to test for a significant difference in estimates of  $b$ .

We repeated this analysis using the entire available dataset regardless of the number of data points available at each time window for both the global suite of high-frequency sensor lakes and the WQP lakes. Fitting the model to unequally sized distributions did not alter any of the trends observed, although the magnitude of the  $b$  coefficient decreased slightly (Figure S4).

We also calculated the magnitude of daily change for both light attenuation ( $\Delta K_d$ ) and euphotic depth ( $\Delta z_{\text{eu}}$ ) as the absolute difference between each day and the previous day, as well as absolute percent change. We also calculated changes for time windows ranging from 1 to 16 days apart, as both a single observation and a cumulative observation. Single observation changes were recorded as the absolute difference between day  $n$  and day 1, where day 1 is the date of original measurement. Cumulative changes were recorded as the sum of all absolute daily changes between day 1 and day  $n$ . We chose 16 days as the upper limit (rather than 61 days) for these analyses because it is the return time of the Landsat satellites and therefore represents a commonly used sampling window.

## Across-lake comparisons

Across the 35 globally distributed lakes, water chemistry and trophic state data were collected at each study lake

using a combination of in situ sensors and laboratory analyses. NEON data was obtained from the NEON data portal for five sites (NEON, 2020a, 2020c). We calculated average values of chlorophyll  $a$ , dissolved organic carbon (DOC), fluorescent dissolved organic matter (fDOM), and turbidity using data from the same time that light data was collected whenever possible. Where this was not possible, long-term means were used if available. We used these data to assess potential optically active substance contributions to variation in water clarity. Specifically, we assessed if water quality or lake attributes (chlorophyll  $a$ , DOC, fDOM, turbidity, catchment area, and residence time) were significant predictors of residuals in Equation (1).

Water chemistry data from the WQP sites were collected as described by Read et al. (2017). We used these data and lake origin classifications (constructed reservoir versus natural lake) to understand potential drivers of differences in Taylor's law coefficients; see supplemental information for further details.

Using high-frequency sensor data from sites with incident above-surface PAR ( $n=9$ ) we calculated the coefficients from Equation (1) (Taylor's law) applied to incident PAR data. We then compared this coefficient with the slope coefficient from high-frequency water clarity data from these same sites. This analyses enabled us to assess if the observed variability in water clarity was purely a function of variation in incident light or whether the variance patterns indicated that water clarity was responsive to other ecological processes.

## RESULTS

We discovered that the relationship between variance in water clarity (measured as the light attenuation coefficient  $K_d$ ,  $\text{m}^{-1}$ ) and mean water clarity was consistent with Taylor's law in both our short-term, high-frequency, and long-term, low-frequency datasets. At high frequencies, the data followed Taylor's law at all time windows ranging from 2 to 61 days across lakes (Figure 1). However, the nature of this relationship changed with the length of time over which water clarity was averaged, and the fit of the linear relationship of log variance to log mean (measured as  $R^2$ ) increased from 0.46 averaging over 2 days to 0.87 averaging over 61 days. Both parameters from Equation (1) ( $a$ ,  $b$ ) significantly increased with the size of the time-averaging window;  $a$  (Spearman's rank correlation,  $\rho=0.99$ ,  $p<0.001$ ) increased from 0.0016 averaging over 2 days to 0.028 averaging over 61 days (Figure 1a), and  $b$  (Spearman's rank correlation,  $\rho=0.85$ ,  $p<0.001$ ) increased from 2.31 averaging over 2 days to 2.76 averaging over 61 days (Figure 1). These coefficients both increased asymptotically and these same patterns were observed whether overlapping or non-overlapping observation windows were used. While  $b$  and  $R^2$  both appear to approach a maximum of about 2.8 and 0.9, respectively,

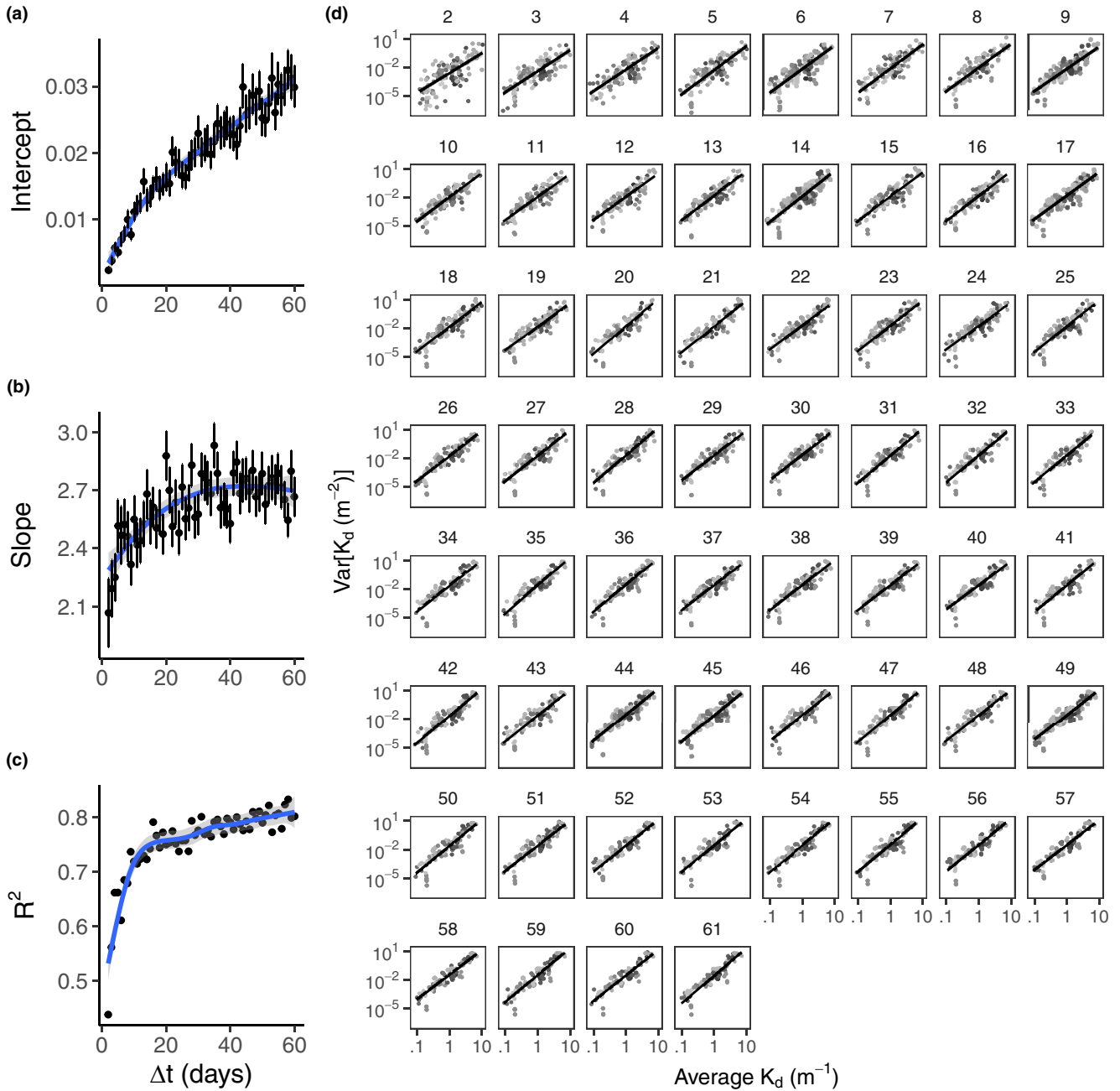


**FIGURE 1** Values of (a)  $a$ , (b)  $b$ , and (c)  $R^2$  for Equation (8) obtained from fitted regressions of log–log plots of the variance in light attenuation versus the mean light attenuation for a moving time window ranging from 2 to 61 days. After applying the moving window to each lake, 30 points were sampled from the time series to avoid overlapping time windows (d) Log–log plots of variance in light attenuation versus the mean light attenuation for time windows ranging from 2 to 61 days (indicated at the top of each plot). Points represent individual samples, and the solid line represents the power function as described by (a), (b), and (c) for all lakes. For all plots in (d)  $n=630$  (30 points each for 21 lakes).

$a$  kept increasing in the 61-day time window. When the variance and mean were calculated over the entire period available for each lake, regardless of differences in the observation length of each lake,  $a$  was 0.09,  $b$  was 2.27 and  $R^2$  was 0.88 (Figure 2). We found no significant relationship between residuals for this relationship and lake or water quality attributes. However, we found that eutrophic and dystrophic lakes had greater absolute residuals than mesotrophic or oligotrophic lakes

(Figure S5) The  $b$  coefficient applied to incident PAR was 1.2, whereas the coefficient for water clarity measurements from these same lakes ( $n=9$ ) was substantially higher (3.0).

Taylor's law was also satisfied using our long-term (defined as a sampling interval of at least 61 days) water clarity data measured in 6342 US lakes (Figure 3a;  $n=6342$  lakes,  $b=2.71$ ,  $R^2=0.81$ ). For these lower-frequency observations, the median number of observations and

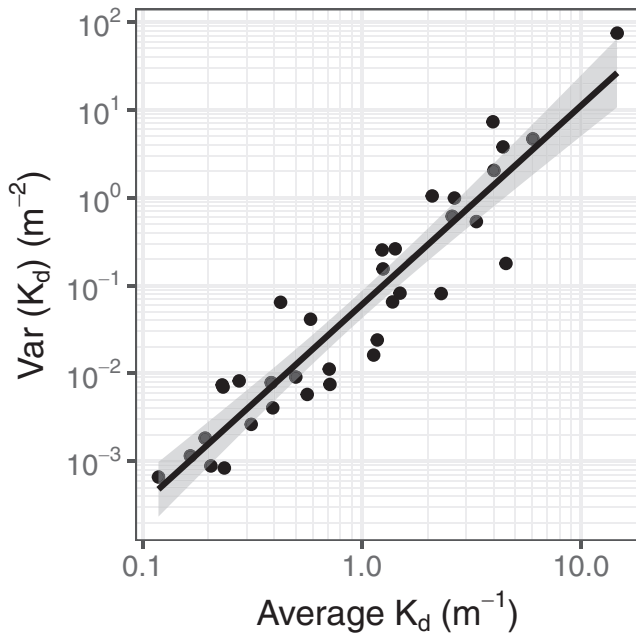


**FIGURE 2** Log–log plot of variance in light attenuation versus the mean light attenuation using the entire time series available for each lake, so that there is only a single data point per lake.  $a=0.09$ ,  $b=2.27$ ,  $R^2=0.88$ .

duration of available water clarity measurements were 48 observations and 12 years per lake, respectively. We also found that  $b$  varied significantly across US geographic regions with  $b$  ranging from 1.95 to 3.01 (Figure 3b–f; Table S2). Similarly,  $b$  was significantly ( $p<0.001$ ) lower for reservoirs ( $b=2.20$ ) than natural lakes ( $b=2.74$ ) (Figure S6).

For the magnitude of daily changes in water clarity, similar to Taylor's law, we found a strong power relationship ( $\Delta K_d=0.10 \mu^{1.1}$ ,  $R^2=0.84$ ,  $p<0.001$ ) between the average daily change in water clarity and the average water clarity coefficient of each lake over the measured timespan (Figure 4a). However, lakes that experienced smaller  $\Delta K_d$  exhibited much greater daily changes in the estimated depth of the euphotic zone (defined as the depth range from the surface to where 1% of surface light remains) (Figure 4b). The relationship between changes in euphotic depth ( $\Delta z_{eu}$ ) and average light attenuation was also described by a power function ( $\Delta z_{eu}=0.56 \mu^{-0.86}$ ,  $R^2=0.68$ ,  $p<0.001$ ). A large  $K_d$  corresponds to a small euphotic zone because light is more rapidly attenuated, but large changes in  $K_d$  do not necessarily represent equally large changes in euphotic depth. For example, the largest single observed daily  $\Delta K_d$  was  $20 \text{ m}^{-1}$  in Hawksbury Lagoon, an extremely shallow, hypertrophic, polymictic lake in New Zealand, which corresponded to a change in euphotic depth of only 0.12m. On the other hand, a  $\Delta K_d$  of just  $0.07 \text{ m}^{-1}$  in Lago Cochrane, a deep oligotrophic lake in Chile, corresponded to a change of 22m in euphotic depth. However, for both lakes, there was a similar change in euphotic depth as a fraction of lake depth (18% and 22% of the mean depth, respectively).

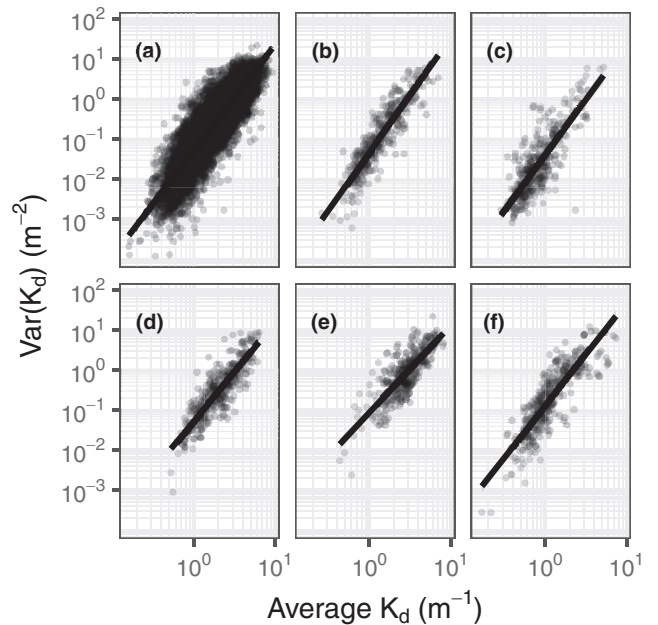


**FIGURE 3** Variance in light attenuation ( $K_d$ ) versus average  $K_d$  calculated from at least 15 Secchi depth measurements spanning at least 61 days in lakes across (a) the entire US national dataset ( $y=0.05x^{2.71}$ ,  $R^2=0.81$ ,  $p<0.001$ ,  $n=6342$ ), (b) the US Midwest ( $y=0.06x^{2.83}$ ,  $R^2=0.86$ ,  $p<0.001$ ,  $n=66$ ), (c) the US Northeast ( $y=0.05x^{3.01}$ ,  $R^2=0.73$ ,  $p<0.001$ ,  $n=66$ ), (d) the US Southeast ( $y=0.06x^{2.32}$ ,  $R^2=0.70$ ,  $p<0.001$ ,  $n=66$ ), (e) the US Southwest ( $y=0.2x^{1.95}$ ,  $R^2=0.66$ ,  $p<0.001$ ,  $n=66$ ), and (f) the US West ( $y=0.1x^{2.30}$ ,  $R^2=0.81$ ,  $p<0.001$ ,  $n=66$ ). For each of the previous equations the null hypothesis, that the slope is equal to zero, was rejected. An equal number of points were sampled from the regions used in (b–f) to avoid the influence of sample size on results.

Daily percent change in water clarity across lakes was highly variable and displayed no discernible pattern (Figure 4c), suggesting that proportionally larger changes are no more frequent in low-clarity lakes than in high-clarity lakes. While large daily changes in water clarity were occasionally observed in most lakes, they were much less common than smaller changes; the median average daily percent change across all lakes was 10% (range: 2%–43%). No trends were observed in relation to different sensor manufacturers, measurement frequency, or number of sampled days. For example, both the second highest (Lake Glubokoe, 38%) and lowest (Lake Gribsoe, 2.0%) average daily percent changes were calculated from Onset sensors measuring at 10-min intervals.

Both cumulative and observed absolute changes in water clarity and euphotic depth increased roughly linearly with time (Figure S7). For example, averaged across the 35 lakes for which high-frequency data were available, the cumulative absolute change in the euphotic zone was 20m at 16days. In contrast, comparing any pairs of days 16days apart, the estimated euphotic zone depth differed by 2.1 m on average, indicating that much of the short-term change in water clarity represents variability around the mean, rather



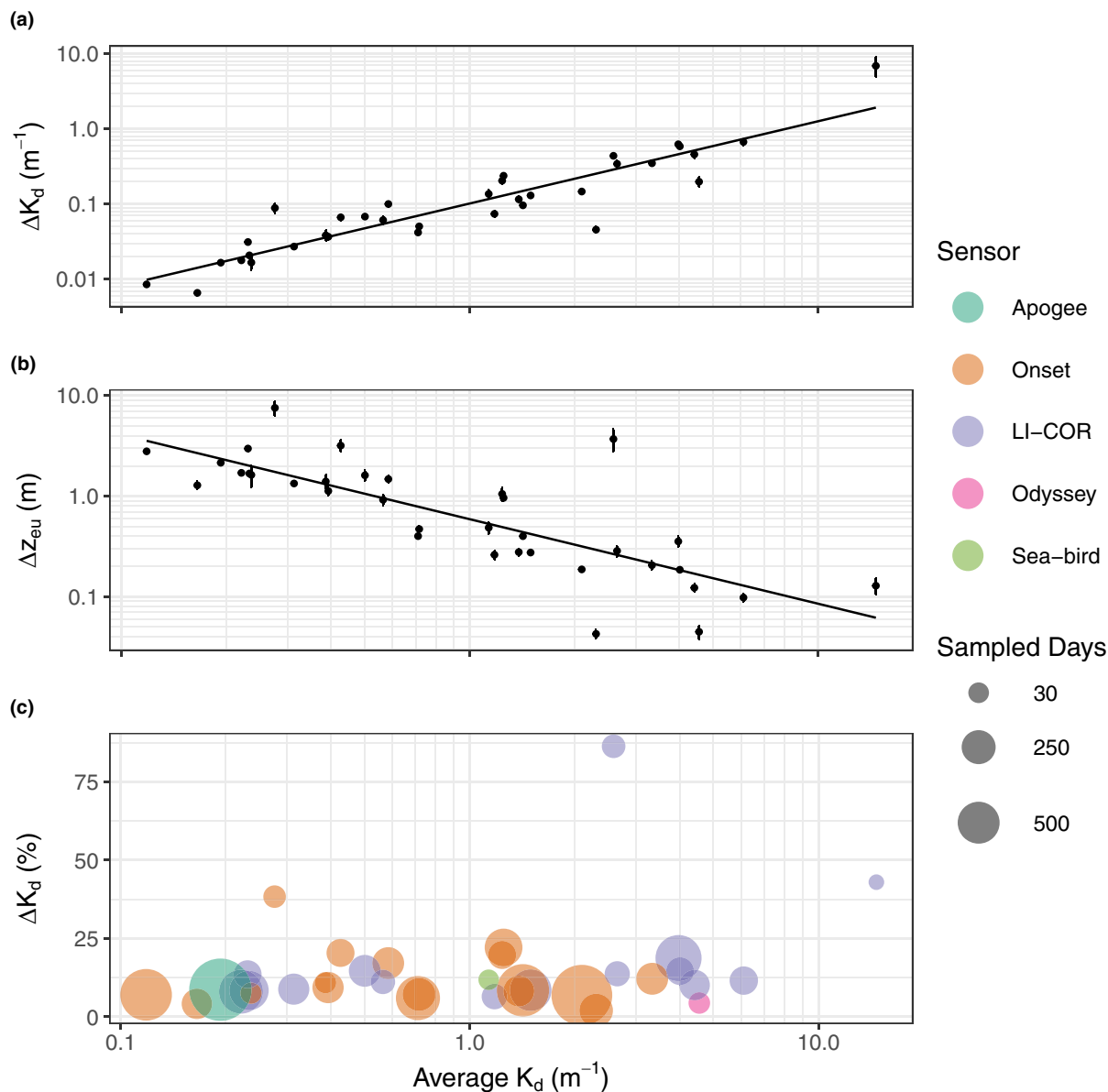


**FIGURE 4** Average daily change (a) in light attenuation ( $K_d$ ) as a magnitude, (b) euphotic depth, and (c) light attenuation as a percent change against average light attenuation for each lake. The euphotic zone represents the depth range over which photosynthesis can occur. Error bars in (a) and (b) represent the standard error in average daily change, and the lines represent the best fitting linear model on log–log coordinates. Linear relationships on log–log plots are equivalent to power functions, and the fitted regressions yield: (a)  $y=0.10\mu^{1.1}$ ,  $R^2=0.84$ ,  $p<0.001$  and (b)  $y=0.56\mu^{-0.86}$ ,  $R^2=0.68$ ,  $p<0.001$ . In (c), colours define the sensors used, and point size represents the number of sampled days.

than consistent directional change. This same general observation held true individually in each of our lakes. To determine how much variability in water clarity would be missed when sampling at different intervals, we calculated the ratio of the observed change in water clarity to the cumulative change in water clarity up to 16 days for each lake except Hawksbury Lagoon, since only 12 days of data were available for this lake (Figure 5). We found that, on average, 50% of the variability in water clarity is missed if the sampling frequency is 3 days, while 75% is missed using a sampling frequency of 8 days.

## DISCUSSION

Using water clarity as an integrative ecological attribute, we demonstrate that ecological variability is consistent with Taylor's law across lakes from days to decades. Furthermore, model coefficients describing the power-law relationship between the mean and variance increase in a predictable way with increasing time intervals, such that the  $b$  coefficient at roughly 2 months ( $b=2.76$ ) is similar to the value observed at a decadal scale ( $b=2.71$ ). Our discovery effectively links the behaviour of variance across many orders

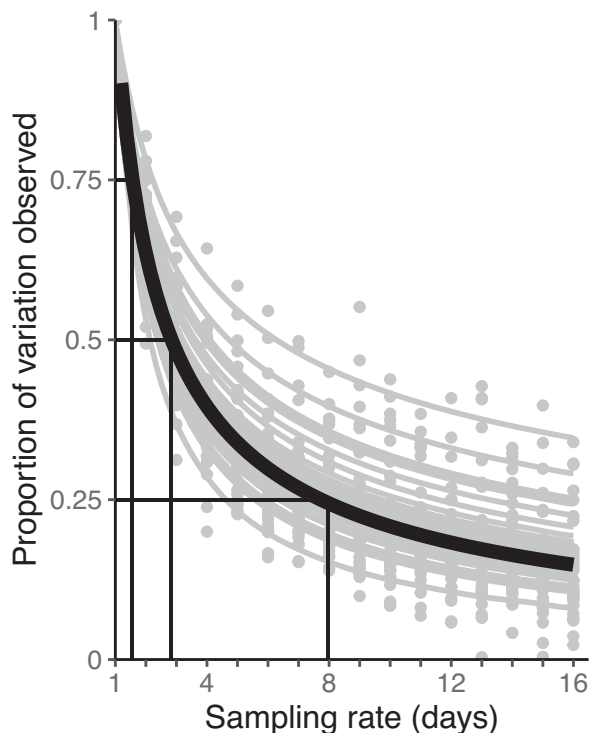


**FIGURE 5** The ratio of daily change in light attenuation measured as a single observation  $n$  days from the original measurement to daily change in light attenuation as a cumulative day-to-day change for all  $n$  days since the original measurement, where  $x=n$  days. Points represent the average ratio for each lake at  $n$  days, and grey lines represent fitted power functions for each lake. The thick black curve represents the average power function applied to all lakes,  $y=x^{-0.67}$ . Thin black lines show the average number of days required for the ratio to reach values of 0.75, 0.5, and 0.25. The  $y$  axis can be interpreted as the proportion of potential daily variation that is observed using the sampling frequency on the  $x$  axis. Hawksbury Lagoon was excluded from this figure since only 12 days of data are available.

of magnitude in water clarity, demonstrating the potential to predict variance at one temporal scale from that observed at another scale. These insights link high-frequency measurements to long-term ecological records. This research is the first we know to test and confirm Taylor's law using high-frequency ecological measurements, which are becoming increasingly available via numerous sensor networks.

Changes in water clarity, despite being mechanistically governed by variation in both biotic and abiotic characteristics (Kirk, 1994; Morris et al., 1995; Rose et al., 2014), exhibit predictable behaviour across a wide range of temporal scales and across sites. Both  $a$  and  $b$  increased with the averaging window used, which is consistent with our explanation of a greater degree of variability and a lack of synchrony across sites at larger time scales (Reuman et al., 2017). The dependence of  $b$  on the size of the averaging window has also been observed in temporal fluctuations in the stock market (Eisler & Kertész, 2006) and complex network traffic (Duch & Arenas, 2006), and in the spatial distribution of urban

facilities (Wu et al., 2019). In the case of stock market fluctuations, Eisler and Kertész (2006) attributed this to the time taken for news reports and policy changes to affect the stock market. Similarly, the observed increase in  $a$  and  $b$  with averaging time in our study demonstrates that variation in water clarity and differences across sites is greater over longer time periods, as expected, and is likely the result of the increased chance of a meteorological or other type of event (e.g., algal bloom) that alters water clarity as well as the influence of seasonal events (e.g., mixing, photobleaching) on water clarity. The substantial difference of the slope coefficient  $b$  between light attenuation ( $b=3.0$ ) and incident above-surface light ( $b=1.2$ ) suggests that different processes regulate the relationship between mean and variance in these two different types of data. However, that time series of two very different phenomena, namely our observations of water clarity and the observations of Eisler and Kertész (2006) of the stock market, both obey Taylor's law in a similar fashion adds to the evidence of one or more broadly applicable underlying mathematical explanations that are independent of the conditions of any particular study system (Cohen, 2019; Eisler et al., 2008; Giometto et al., 2015; Xiao et al., 2015).

Additionally, we show that across all time windows,  $b$  is always greater than two, which is higher than many, but not all, observations of Taylor's law (Eisler et al., 2008; Giometto et al., 2015). One explanation for this is that water clarity measurements may be relatively autocorrelated, as we also found that the increase in  $b$  with averaging time corresponded with increased autocorrelation in the averaged water clarity time series. This hypothesis is consistent with previous research that suggested increasing temporal autocorrelation can lead to greater  $b$  estimates (Xu & Cohen, 2021). The degree of autocorrelation may also explain geographic variability in  $b$  coefficients (Figure 3), but we have not tested that possibility.

The difference in  $b$  calculated from our high-frequency versus low-frequency observations suggests that although variance in water clarity exhibits clear patterns consistent with Taylor's law, ecological heterogeneity across regions, lake types, and through time in individual lakes still plays an important role in regulating variability in water clarity. For example, across regions of the United States we see that  $b$  is largest in the north (Northeast, Midwest), lower in the south (Southeast, Southwest), and intermediate in the west (West). A possible explanation for this may be that lakes in northern or mountainous regions experience greater seasonality than those in the south, resulting in a wider range of water clarity values. These results are consistent with Soranno et al. (2019), who found that regional and local spatial drivers such as land use and land cover in catchment watersheds, regional climate, and lake morphology, had a greater effect on total variation in lake ecosystem properties than temporal effects. Similarly, our results showing that variance

increases with the mean faster in natural lakes than in reservoirs demonstrate how lake attributes influence variance patterns. Further research is needed to identify specific factors controlling these differences, which could result from the fact that reservoirs are more heavily managed and also often dominated by different optically active substances than natural lakes. Regardless, our results indicate that across a wide variety of geographic regions and climates, land use and land cover types, and morphological characteristics (Table 1), variation in lake water clarity at both short- and long-term time scales is largely generalizable using only the average water clarity and the amount of variability measured over any given period of time.

While variation in water clarity was consistent with Taylor's law across lakes, the high-frequency time series for individual lakes exhibited variance patterns that were not always consistent with Taylor's law. One reason for this is that even for the largest time window of 61 days, the range of observed water clarity measurements, and hence variance, was relatively small and rarely exceeded an order of magnitude across the observation period. In contrast, across lakes, average water clarity spanned several orders of magnitude (Figure 2). In the few cases where water clarity in an individual lake spanned a complete or near-complete order of magnitude during the observation period (Prairie Lake, Prairie Pothole, and Buffalo Pound), the data were consistent with Taylor's law (Figure S3). This agrees with previous studies that have assessed the limitation of small data sets or small variation in measurements on Taylor's law bias (Clark & Perry, 1995). It is likely that within most individual lakes and at the temporal scale of days to seasons, the range of water clarity variability is not large enough to warrant applying Taylor's law individually, absent a substantial event that greatly alters water clarity. This implies that for most lakes, a long-term estimate of water clarity may be sufficient to estimate potential short-term variance based on the relationship observed across lakes.

For most lakes, it was difficult to identify the specific sources of variation in water clarity from the data we collected. It is well known that water clarity is primarily governed by optically active substances including algal biomass, dissolved substances, and inorganic suspended solids (Kirk, 1994; Rose et al., 2014), and can be influenced by meteorological events (Anthony et al., 2004; Perga et al., 2018). Our findings are consistent with past studies showing that both dissolved organic matter and algal biomass (as measured by chlorophyll *a* concentrations) are important in regulating water clarity (Figure S8). While we did not identify specific drivers of variations in clarity in most lakes, we observed strong relationships between variance in water clarity and the average concentrations of optically active substances (Figure S9). The Taylor's law slope coefficient *b* (from Equation 1) also did not differ between lakes where algal biomass dominated water clarity versus lakes where

non-algal particulates dominated water clarity ( $p=0.115$ ; Figure S10). However, the intercept *a* for the non-algal lakes was larger than the intercept for algal lakes, and hence the overall variance was larger in the non-algal lakes. Additionally, although the sample sizes are small, eutrophic and dystrophic lakes appeared to have greater absolute residuals for Equation (1) (Figure S5). These results reinforce the important role that substances including dissolved organic matter and algal biomass play in regulating variability in water clarity. Further research is needed to assess if individual differences in Taylor's law slope coefficients among lakes are associated with differences in optically active substances, or if variability is changing over time.

Our results show that a substantial amount of temporal variation is missed when water clarity is coarsely sampled. For example, we found that sampling water clarity every 16 days, which corresponds to the frequency of the return time of Landsat satellites, misses over 75% of the variation in water clarity (Figure 5; Figure S7). Many researchers suggest gathering in situ data within 3 days of a satellite overpass as validation for remote sensing estimates (Kuhn et al., 2019; Olmanson et al., 2008). However, our findings suggest that euphotic depth, and similarly Secchi depth, potentially differs by over 2 m on average over the course of 3 days in oligotrophic lakes.

Variations in water clarity are ecologically important. Daily changes in water clarity and euphotic depth were typically low (the median daily change was less than 13% of the maximum in half of the sampled lakes). However, our results indicate that the low variation in light attenuation observed in clearer lakes often corresponds to higher variation in euphotic depth and Secchi depth. Because the euphotic zone regulates the depth range over which primary production can occur, large variations in water clarity are likely to quickly alter patterns in productivity (e.g., Leach et al., 2017). Changes in water clarity also alter how zooplankton behaviorally respond to threats from ultraviolet radiation and fish predation pressure (Williamson et al., 2011) and water clarity is a key factor regulating fish species distribution (Ferguson, 1958). Additionally, because water clarity regulates how heat is absorbed in the water column, variation in water clarity also impacts temperature and dissolved oxygen dynamics in lakes (Perga et al., 2023). Scaling relationships are a fundamental component of ecological theory, but their application to highly dynamic ecosystems depends on quantifying variance appropriately (Savage, 2004). Our results advance the current understanding of light variance in lakes, which may lend itself to the application of other scaling relationships to lake ecosystems. Understanding the relationship between mean and variance in water clarity, and for more ecological variables in a variety of ecosystems, will enable researchers to quantify patterns of variability and heterogeneity across time and space.

To our knowledge, this study represents the largest collection of high-frequency water clarity measurements to date and covers a wide range of lake ecosystems and geographical regions. Our results demonstrate the value of integrating data measured across diverse temporal scales from days to decades, and across regional to global extents. Our findings also highlight the benefits of high-frequency measurements to supplement more conventional lower frequency (e.g., monthly to annual) measurements, and the possibility of estimating variability at longer time scales (e.g., years to decades) from daily measurements. While our research focused only on water clarity in lakes, similar methods applied to other ecological variables could greatly expand insights into the scaling of variance at landscape and macrosystem scales. However, our results also demonstrate that Taylor's law cannot be blindly applied to predict ecological variation at longer time scales from short-term measurements. Variance patterns in individual lakes were not consistent with Taylor's law unless they exhibited variability of at least an order of magnitude, and the relationship across lakes depends on the averaging window because the variance increases with time. These insights improve the ability to integrate ecological data collected across highly variable spatial or temporal scales and may improve understanding of macrosystems phenomena from site-based research.

## AUTHOR CONTRIBUTIONS

MRG and KCR designed the study and drafted the manuscript. MRG analysed the data. All authors contributed to data collection, data interpretation, and/or editing the manuscript. Aside from MRG and KCR, author order is alphabetical.

## AFFILIATIONS

<sup>1</sup>Department of Biological Sciences, Rensselaer Polytechnic Institute, Troy, New York, USA

<sup>2</sup>Laboratório de Limnologia, Ecotoxicologia e Ecologia Aquática (LIMNEA), Instituto de Ciências Biológicas (ICB), Universidade Federal de Minas Gerais, Belo Horizonte, Minas Gerais, Brazil

<sup>3</sup>Centre for Freshwater and Environmental Studies, Dundalk Institute of Technology, Louth, Ireland

<sup>4</sup>School of Environment and Sustainability and Global Institute for Water Security, University of Saskatchewan, Saskatoon, Saskatchewan, Canada

<sup>5</sup>Universidade do Estado de Minas Gerais (UEMG), Divinópolis, Minas Gerais, Brazil

<sup>6</sup>Physics of Aquatic Systems Laboratory, Margaretha Kamprad Chair, Lausanne, École Polytechnique Fédérale de Lausanne, Lausanne, Switzerland

<sup>7</sup>Eusserthal Ecosystem Research Station (EERES), Institute for Environmental Sciences (IES), University of Kaiserslautern-Landau (RPTU), Landau, Germany

<sup>8</sup>Laboratory of Populations, The Rockefeller University, New York, New York, USA

<sup>9</sup>Department of Statistics and Earth Institute, Columbia University, New York, New York, USA

<sup>10</sup>Department of Statistics, University of Chicago, Chicago, Illinois, USA

<sup>11</sup>Marine Institute, Furnace, Newport, Co. Mayo, Ireland

<sup>12</sup>Department of Hydrology, Lomonosov Moscow State University, Moscow, Russia

<sup>13</sup>UK Centre for Ecology and Hydrology, Lancaster Environment Centre, Lancaster, UK

<sup>14</sup>Department of Sustainable Agro-ecosystems and Bioresources, Research and Innovation Centre, Fondazione Edmund Mach, San Michele all'Adige, Italy

<sup>15</sup>Department of Cybernetics, School of Science, Tallinn University of Technology, Tallinn, Estonia

<sup>16</sup>Australian Rivers Institute, Griffith University, Brisbane, Queensland, Australia

<sup>17</sup>Département de Géomatique Appliquée, Université de Sherbrooke, Sherbrooke, Quebec, Canada

<sup>18</sup>IBM Research, Yorktown Heights, New York, USA

<sup>19</sup>Inland Fisheries Ireland, Dublin, Ireland

<sup>20</sup>Chair of Hydrobiology and Fishery, Institute of Agricultural and Environmental Science, Estonian University of Life Sciences, Tartu, Estonia

<sup>21</sup>Department of Remote Sensing and Marine Optics, Estonian Marine Institute, University of Tartu, Tallinn, Estonia

<sup>22</sup>Environmental Research Institute, University of Waikato, Hamilton, New Zealand

<sup>23</sup>Aquatic Physics Group, Department F.-A. Forel for Environmental and Aquatic Sciences (DEFSE), Faculty of Science, University of Geneva, Geneva, Switzerland

<sup>24</sup>Faculty of Geoscience and Environment, University of Lausanne, Lausanne, Switzerland

<sup>25</sup>Centro de Investigación en Ecosistemas de la Patagonia (CIEP), Coyhaique, Chile

<sup>26</sup>National Ecological Observatory Network, Boulder, Colorado, USA

<sup>27</sup>Department of Ecoscience, Aarhus University, Roskilde, Denmark

<sup>28</sup>Nordic Harvest, Taastrup, Denmark

<sup>29</sup>Lakes Alliance, Belgrade Lakes, Maine, USA

<sup>30</sup>Lake City Field Station, Minnesota Department of Natural Resources, Lake City, Minnesota, USA

## ACKNOWLEDGEMENTS

We acknowledge the Global Lake Ecological Observatory Network for providing the collaborative platform to enable this research. MRG and KCR acknowledge support from US National Science Foundation grants 1655168, 1638704, 1754265, and 1761805, US AID grant Award 72067419FA00001, a New York State Higher Education Capital grant (#7290), and assistance by personnel associated with the Jefferson Project at Lake George, a collaboration between Rensselaer Polytechnic Institute, IBM Research and the Lake George Association. Data collection at Blelham Tarn and Windermere was supported by Natural Environment Research Council award number NE/R016429/1 as part of the UK-SCaPE programme delivering National Capability. MRA and SK were supported as part of the BEYOND 2020 project (grant-aid agreement no. PBA/FS/16/02) by the Marine Institute and funded under the Marine Research Programme by the Irish Government. JEC thanks Roseanne Benjamin for her help during this work. BLR would like to thank the Dirección General de Aguas XI Region of Chile for contributing to sensors and maintenance of the buoy in Lago Cochrane and support from ANID R20F0002 project PATSER. Data collection from Carioca and Dom Helvécio was supported by Long-Term Ecological Research/National Research Council—CNPq (No. 403698/2012-0). AL and data from Estonian lakes were supported by the Estonian Research Council grants (PSG32, PRG1167, and PRG709). AG was supported by grants PRG119 and EMP480. Data collection at Chavonnes and Lioson was supported by the Swiss National Science Foundation (SNSF grant No.

200021\_169899, Methane Paradox). Data collection from Buffalo Pound Lake was supported by the Canada Foundation for Innovation, Global Water Futures and FORMBLOOM the National Science and Engineering Research Council, and Buffalo Pound Water Treatment Plant. For data from Lake Geneva, we acknowledge the technical team of the LÉXPLORE platform and the LÉXPLORE five partner institutions: Eawag, EPFL, University of Geneva, University of Lausanne, and CARTELL (INRAE-USMB). The National Ecological Observatory Network is a program sponsored by the National Science Foundation and operated under a cooperative agreement by Battelle. This material is based in part upon work supported by the National Science Foundation through the NEON Program. Data from Lake Tovel (LTER\_EU\_IT\_090) was supported by the Fondazione Edmund Mach, Italy.

## PEER REVIEW

The peer review history for this article is available at <https://www.webofscience.com/api/gateway/wos/peer-review/10.1111/ele.14451>.

## DATA AVAILABILITY STATEMENT

Raw high-frequency data used in this study have been made publicly available via Environmental Data Initiative (<https://doi.org/10.6073/pasta/85daa83c2fe8e3079cce503b747a7255>). Raw Secchi depth data was taken from the Water Quality Portal (<https://doi.org/10.5066/P9QRKUVJ>).

## ORCID

Max R. Glines  <https://orcid.org/0000-0002-9911-6841>

## REFERENCES

- Adrian, R., O'Reilly, C.M., Zagarese, H., Baines, S.B., Hessen, D.O., Keller, W. et al. (2009) Lakes as sentinels of climate change. *Limnology and Oceanography*, 54(6, Part 2), 2283–2297. Available from: [https://doi.org/10.4319/lo.2009.54.6\\_part\\_2.2283](https://doi.org/10.4319/lo.2009.54.6_part_2.2283)
- Anthony, K.R.N., Ridd, P.V., Orpin, A.R., Larcombe, P. & Lough, J. (2004) Temporal variation of light availability in coastal benthic habitats: Effects of clouds, turbidity, and tides. *Limnology and Oceanography*, 49(6), 2201–2211. Available from: <https://doi.org/10.4319/lo.2004.49.6.2201>
- Briegleb, B.P., Minnis, P., Ramanathan, V. & Harrison, E. (1986) Comparison of regional clear-sky albedos inferred from satellite observations and model computations. *Journal of Climate and Applied Meteorology*, 25(2), 214–226. Available from: [https://doi.org/10.1175/1520-0450\(1986\)025<0214:CORCSA>2.0.CO;2](https://doi.org/10.1175/1520-0450(1986)025<0214:CORCSA>2.0.CO;2)
- Clark, S.J. & Perry, J.N. (1995) Small sample estimation for Taylor's power law. *Environmental and Ecological Statistics*, 302(1994), 287–302. Available from: <https://doi.org/10.1007/BF00469426>
- Cohen, J.E. (2014) Taylor's law and abrupt biotic change in a smoothly changing environment. *Theoretical Ecology*, 7(1), 77–86. Available from: <https://doi.org/10.1007/s12080-013-0199-z>
- Cohen, J.E. (2019) Every variance function, including Taylor's power law of fluctuation scaling, can be produced by any location-scale family of distributions with positive mean and variance. *Theoretical Ecology*, 13, 1–5. Available from: <https://doi.org/10.1007/s12080-019-00445-7>
- Cohen, J.E. & Xu, M. (2015) Random sampling of skewed distributions implies Taylor's power law of fluctuation scaling. *Proceedings of the National Academy of Sciences of the United States of America*, 112(25), 7749–7754. Available from: <https://doi.org/10.1073/pnas.1503824112>
- Collins, S.L., Avolio, M.L., Gries, C., Hallett, L.M., Koerner, S.E., La Pierre, K.J. et al. (2018) Temporal heterogeneity increases with spatial heterogeneity in ecological communities. *Ecology*, 99(4), 858–865. Available from: <https://doi.org/10.1002/ecy.2154>
- Downing, J.A. (1986) Spatial heterogeneity: evolved behaviour or mathematical artefact? *Nature*, 323(18), 255–257. Available from: <https://doi.org/10.1038/323255a0>
- Duch, J. & Arenas, A. (2006) Scaling of fluctuations in traffic on complex networks. *Physical Review Letters*, 96(21), 1–4. Available from: <https://doi.org/10.1103/PhysRevLett.96.218702>
- Eisler, Z. & Kertész, J. (2006) Scaling theory of temporal correlations and size-dependent fluctuations in the traded value of stocks. *Physical Review E-Statistical, Nonlinear, and Soft Matter Physics*, 73(4), 1–7. Available from: <https://doi.org/10.1103/PhysRevE.73.046109>
- Eisler, Z., Bartos, I. & Kertész, J. (2008) Fluctuation scaling in complex systems: Taylor's law and beyond. *Advances in Physics*, 57(1), 89–142. Available from: <https://doi.org/10.1080/00018730801893043>
- Ferguson, R.G. (1958) The preferred temperature of fish and their midsummer distribution in temperate lakes and streams. *Journal of the Fisheries Board of Canada*, 15(4), 607–624. Available from: <https://doi.org/10.1139/f58-032>
- Gardner, J.R., Ensign, S.H., Houser, J.N. & Doyle, M.W. (2020) Light exposure along particle flowpaths in large rivers. *Limnology and Oceanography*, 65(1), 128–142. Available from: <https://doi.org/10.1002/lno.11256>
- Giometto, A., Formentin, M., Rinaldo, A., Cohen, J.E. & Maritan, A. (2015) Sample and population exponents of generalized Taylor's law. *Proceedings of the National Academy of Sciences of the United States of America*, 112(25), 7755–7760. Available from: <https://doi.org/10.1073/pnas.1505882112>
- Heino, J., Alahuhta, J., Bini, L.M., Cai, Y., Heiskanen, A.S., Hellsten, S. et al. (2021) Lakes in the era of global change: moving beyond single-lake thinking in maintaining biodiversity and ecosystem services. *Biological Reviews*, 96(1), 89–106. Available from: <https://doi.org/10.1111/brv.12647>
- Kilpatrick, A.M. & Cruz, S. (2014) Species interactions can explain Taylor's power law for ecological time series. *Nature*, 422, 65–68. Available from: <https://doi.org/10.1038/nature01471>
- Kirk, J.T.O. (1994) *Light and photosynthesis in aquatic ecosystems*. Cambridge: Cambridge University Press. Available from: <https://doi.org/10.1017/CBO9780511623370>
- Kuhn, C., de Matos, A., Ward, N., Loken, L., Oliveira, H., Kampel, M. et al. (2019) Performance of Landsat-8 and Sentinel-2 surface reflectance products for river remote sensing retrievals of chlorophyll-a and turbidity. *Remote Sensing of Environment*, 224, 104–118. Available from: <https://doi.org/10.1016/j.rse.2019.01.023>
- Leach, T.H., Beisner, B.E., Carey, C.C., Pernica, P., Rose, K.C., Huot, Y. et al. (2017) Patterns and drivers of deep chlorophyll maxima structure in 100 lakes: the relative importance of light and thermal stratification. *Limnology and Oceanography*, 63, 628–646. Available from: <https://doi.org/10.1002/lno.10656>
- Levin, S.A. (1992) The problem of pattern and scale in ecology. *Ecology*, 73(6), 1943–1967. Available from: <https://doi.org/10.2307/1941447>
- Long, M.H., Rheuban, J.E., Berg, P. & Ziemann, J.C. (2012) A comparison and correction of light intensity loggers to photosynthetically active radiation sensors. *Limnology and Oceanography: Methods*, 10, 416–424. Available from: <https://doi.org/10.4319/lom.2012.10.416>
- Lottig, N.R., Wagner, T., Henry, E.N., Cheruvilil, K.S., Webster, K.E., Downing, J.A. et al. (2014) Long-term citizen-collected

- data reveal geographical patterns and temporal trends in lake water clarity. *PLoS One*, 9(4), 1–12. Available from: <https://doi.org/10.1371/journal.pone.0095769>
- Meinson, P., Idrizaj, A., Noges, P., Noges, T. & Laas, A. (2016) Continuous and high-frequency measurements in limnology: history, applications, and future challenges. *Environmental Reviews*, 24(1), 52–62. Available from: <https://doi.org/10.1139/er-2015-0030>
- Morris, D.P., Zagarese, H., Williamson, C.E., Balseiro, E.G., Hargreaves, B.R., Modenutti, B. et al. (1995) The attenuation of solar UV radiation in lakes and the role of dissolved organic carbon. *Limnology and Oceanography*, 40(8), 1381–1391. Available from: <https://doi.org/10.4319/lo.1995.40.8.1381>
- NEON (National Ecological Observatory Network). (2020a) Photosynthetically active radiation (PAR) (DPI.00024.001). Available from: <https://data.neonscience.org> [Accessed February 7, 2020].
- NEON (National Ecological Observatory Network). (2020b) Photosynthetically active radiation below water surface (DPI.20261.001). Available from: <https://data.neonscience.org> [Accessed February 7, 2020].
- NEON (National Ecological Observatory Network). (2020c) Water quality (DPI.20288.001). Available from: <https://data.neonscience.org> [Accessed February 7, 2020].
- Olmanson, L.G., Bauer, M.E. & Brezonik, P.L. (2008) A 20-year Landsat water clarity census of Minnesota's 10,000 lakes. *Remote Sensing of Environment*, 112, 4086–4097. Available from: <https://doi.org/10.1016/j.rse.2007.12.013>
- Padial, A.A. & Thomaz, S.M. (2008) Prediction of the light attenuation coefficient through the Secchi disk depth: empirical modeling in two large Neotropical ecosystems. *Limnology*, 9, 143–151. Available from: <https://doi.org/10.1007/s10201-008-0246-4>
- Paulson, C.A. & Pegau, W.S. (2001) Penetrating shortwave radiation. *Encyclopedia of Ocean Sciences*, 4, 379–384. Available from: <https://doi.org/10.1016/B978-012374473-9.00154-5>
- Perga, M.E., Minaudo, C., Doda, T., Arthaud, F., Beria, H., Chmiel, H.E. et al. (2023) Near-bed stratification controls bottom hypoxia in ice-covered alpine lakes. *Limnology and Oceanography*, 68(6), 1232–1246. Available from: <https://doi.org/10.1002/lno.12341>
- Perga, M.E., Bruel, R., Rodriguez, L., Guénand, Y. & Bouffard, D. (2018) Storm impacts on alpine lakes: Antecedent weather conditions matter more than the event intensity. *Global Change Biology*, 24(10), 5004–5016. Available from: <https://doi.org/10.1111/gcb.14384>
- Perry, J.N. (1994) Chaotic dynamics can generate Taylor's power law. *Proceedings of the Royal Society of London B*, 257, 221–226. Available from: <https://doi.org/10.1098/rspb.1994.0118>
- Read, E.K., Carr, L., De Cicco, L., Dugan, H.A., Hart, J.A., Kreft, J. et al. (2017) Water quality data for national-scale aquatic research: The Water Quality Portal. *Water Resources Research*, 53, 1735–1745. Available from: <https://doi.org/10.1002/2016WR019993>
- Reuman, D.C., Zhao, L., Sheppard, L.W., Reid, P.C. & Cohen, J.E. (2017) Synchrony affects Taylor's law in theory and data. *PNAS*, 114(26), 6788–6793. Available from: <https://doi.org/10.1073/pnas.1703593114>
- Rose, K.C., Graves, R.A., Hansen, W.D., Harvey, B.J., Qiu, J., Wood, S.A. et al. (2017) Historical foundations and future directions in macrosystems ecology. *Ecology Letters*, 20(2), 147–157. Available from: <https://doi.org/10.1111/ele.12717>
- Rose, K.C., Weathers, K.C., Hetherington, A.L. & Hamilton, D.P. (2016) Insights from the Global Lake Ecological Observatory Network (GLEON). *Inland Waters*, 6(4), 476–482. Available from: <https://doi.org/10.1080/iw-6.4.1051>
- Rose, K.C., Winslow, L.A., Read, J.S., Read, E.K., Solomon, C.T., Adrian, R. et al. (2014) Improving the precision of lake ecosystem metabolism estimates by identifying predictors of model uncertainty. *Limnology and Oceanography: Methods*, 12, 303–312. Available from: <https://doi.org/10.4319/lom.2014.12.303>
- Rusak, J.A., Tanentzap, A.J., Klug, J.L., Rose, K.C., Hendricks, S.P., Jennings, E. et al. (2018) Wind and trophic status explain within and among-lake variability of algal biomass. *Limnology and Oceanography Letters*, 3(6), 409–418. Available from: <https://doi.org/10.1002/lo2.10093>
- Savage, V.M. (2004) Improved approximations to scaling relationships for species, populations, and ecosystems across latitudinal and elevational gradients. *Journal of Theoretical Biology*, 227(4), 525–534. Available from: <https://doi.org/10.1016/j.jtbi.2003.11.030>
- Scheffer, M., Carpenter, S., Foley, J.A., Folke, C. & Walker, B. (2001) Catastrophic shifts in ecosystems. *Nature*, 413(6856), 591–596. Available from: <https://doi.org/10.1038/35098000>
- Soranno, P.A., Wagner, T., Collins, S.M., Lapiere, J.F., Lottig, N.R. & Oliver, S.K. (2019) Spatial and temporal variation of ecosystem properties at macroscales. *Ecology Letters*, 22(10), 1587–1598. Available from: <https://doi.org/10.1111/ele.13346>
- Taylor, L.R. (1961) Aggregation, variance, and the mean. *Nature*, 1, 732–735. Available from: <https://doi.org/10.1038/189732a0>
- Taylor, L.R. & Taylor, R.A.J. (1977) Aggregation, migration and population mechanics. *Nature*, 265(5593), 415–421. Available from: <https://doi.org/10.1038/265415a0>
- Taylor, R.A.J. (2019) *Taylor's power law: order and pattern in nature*. London, UK: Academic Press.
- Williamson, C.E., Fischer, J.M., Bollens, S.M., Overholt, E.P. & Breckenridge, J.K. (2011) Toward a more comprehensive theory of zooplankton diel vertical migration: integrating ultraviolet radiation and water transparency into the biotic paradigm. *Limnology and Oceanography*, 56(5), 1603–1623. Available from: <https://doi.org/10.4319/lo.2011.56.5.1603>
- Williamson, C.E., Saros, J.E., Vincent, W.F. & Smol, J.P. (2009) Lakes and reservoirs as sentinels, integrators, and regulators of climate change. *Limnology and Oceanography*, 54(6 Part 2), 2273–2282. Available from: [https://doi.org/10.4319/lo.2009.54.6\\_part\\_2.2273](https://doi.org/10.4319/lo.2009.54.6_part_2.2273)
- Wu, L., Gong, C. & Yan, X. (2019) Taylor's power law and its decomposition in urban facilities. *Royal Society Open Science*, 6(3), 180770. Available from: <https://doi.org/10.1098/rsos.180770>
- Xiao, X., Locey, K.J. & White, E.P. (2015) A process-independent explanation for the general form of Taylor's law. *American Naturalist*, 186(2), E51–E60. Available from: <https://doi.org/10.1086/682050>
- Xu, M. & Cohen, J.E. (2021) Spatial and temporal autocorrelations affect Taylor's law for US county populations: descriptive and predictive models. *PLoS One*, 16, 1–21. Available from: <https://doi.org/10.1371/journal.pone.0245062>
- Zheng, X., Dickey, T. & Chang, G. (2002) Variability of the downwelling diffuse attenuation coefficient with consideration of inelastic scattering. *Applied Optics*, 41(30), 6477–6488. Available from: <https://doi.org/10.1364/ao.41.006477>

## SUPPORTING INFORMATION

Additional supporting information can be found online in the Supporting Information section at the end of this article.

**How to cite this article:** Glines, M.R., Amancio, R.C.H., Andersen, M.R., Baulch, H., Brighenti, L.S., Chmiel, H.E. et al. (2024) Coefficients in Taylor's law increase with the time scale of water clarity measurements in a global suite of lakes. *Ecology Letters*, 27, e14451. Available from: <https://doi.org/10.1111/ele.14451>